

# Recurrent Action Transformer with Memory

Egor Cherepanov<sup>1\*</sup> Alexey Staroverov<sup>1\*</sup>  
 Dmitry Yudin<sup>1,2</sup> Alexey K. Kovalev<sup>1,2</sup> Aleksandr I. Panov<sup>1,2</sup>  
<sup>1</sup>AIRI, Moscow, Russia, <sup>2</sup>MIPT, Dolgoprudny, Russia  
 {cherepanov, staroverov, yudin, kovalev, panov}@airi.net

## Abstract

Recently, the use of transformers in offline reinforcement learning has become a rapidly developing area. This is due to their ability to treat the agent’s trajectory in the environment as a sequence, thereby reducing the policy learning problem to sequence modeling. In environments where the agent’s decisions depend on past events (POMDPs), capturing both the event itself and the decision point in the context of the model is essential. However, the quadratic complexity of the attention mechanism limits the potential for context expansion. One solution to this problem is to enhance transformers with memory mechanisms. This paper proposes a Recurrent Action Transformer with Memory (RATE), a novel model architecture incorporating a recurrent memory mechanism designed to regulate information retention. To evaluate our model, we conducted extensive experiments on memory-intensive environments (ViZDoom-Two-Colors, T-Maze, Memory Maze, Minigrid.Memory), classic Atari games and MuJoCo control environments. The results show that using memory can significantly improve performance in memory-intensive environments while maintaining or improving results in classic environments. We hope our findings will stimulate research on memory mechanisms for transformers applicable to offline reinforcement learning.

## 1 Introduction

Transformers [49], originally developed for natural language processing (NLP), perform well in Reinforcement Learning (RL) [32, 1]: on-line RL [37, 29, 20, 58, 33, 48, 40], offline RL [11, 26, 30, 27], and model-based RL [10, 34, 43], including for solving credit assignment problems and working in memory-intensive environments [11, 35, 22], provided that the entire trajectory fits within the model context. Transformers struggle with long sequences due to quadratic attention complexity, limiting their use in episodic and continuing tasks. Various approaches attempt to increase context size [16, 55, 7, 14, 8, 17], but such models may become unstable when training on long sequences [56] or to use a specific sparse attention mechanism which is unsuitable for non-NLP tasks [55, 7, 17]. Memory mechanisms offer a promising solution to consider past information without increasing context size. Our work explores memory in transformers for RL, inspired by NLP findings [8]. The RL setting differs from NLP in input sequence processing,

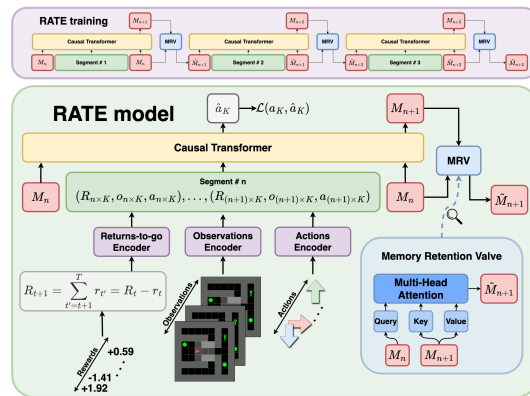


Figure 1: Recurrent Action Transformer with Memory.

Memory mechanisms offer a promising solution to consider past information without increasing context size. Our work explores memory in transformers for RL, inspired by NLP findings [8]. The RL setting differs from NLP in input sequence processing,

\*Equal contribution. The code is available at <https://github.com/AIRI-Institute/RATE>.

requiring specialized encoders for observations, rewards, and actions, and are also characterized by significantly longer sequence lengths during inference.

In RL, memory has 2 senses. One is using past information within an episode to make decisions [29, 35]. The other is transferring experience from one environment to another [33, 48, 28], improving generalizability and solving Meta-RL [50, 19] tasks. Our work focuses on the first sense [35]: using past information to make decisions within the same episode.

In our work, we propose the **Recurrent Action Transformer with Memory (RATE)**, Figure 1), a model that uses memory mechanism: memory embeddings and **Memory Retention Valve (MRV)**. We empirically show that memory embeddings effectively preserve information from previous steps, allowing the model to use past information when making decisions in the present. MRV is designed to control the process of updating memory embeddings and prevent the loss of important information when processing long sequences. We conduct thorough experiments on the memory-intensive environments [46, 38, 12, 35] and on the standard RL benchmarks [6, 21]. We also study the impact of memory on the performance of the proposed model.

Our contribution can be summarized as follows:

1. We propose the Recurrent Action Transformer with Memory (RATE), a transformer model that uses a memory mechanism.
2. We showed that RATE significantly outperforms counterparts without memory mechanism in memory-intensive environments: ViZDoom-Two-Colors, MemoryMaze, Minigrid.Memory and T-Maze.
3. We showed that RATE demonstrates better or comparable results in classic Atari games and MuJoCo control tasks. These tasks do not require the use of memory explicitly, demonstrating that the proposed mechanism is suitable for different types of tasks and emphasizing its universality.

## 2 Background

### 2.1 Offline Reinforcement Learning

In reinforcement learning [47], we assume that the task can be described by a Markov Decision Process as a tuple  $\langle \mathcal{S}, \mathcal{A}, \mathcal{P}, \mathcal{R} \rangle$ . The process consists of states  $s \in \mathcal{S}$ , actions  $a \in \mathcal{A}$ , a state transition function  $\mathcal{P}(s'|s, a)$ , and an immediate reward function  $r = \mathcal{R}(s, a)$ . The states are assumed to have the Markov Property, that is  $\mathbb{P}(s_{t+1}|s_t) = \mathbb{P}(s_{t+1}|s_1, \dots, s_t)$ . Given a timestep  $t$ , we use  $r_t = R(s_t, a_t)$  to denote the immediate reward that the agent receives at state  $s_t$  performing action  $a_t$  at that timestep. We describe trajectory  $\tau$  of length  $T$  as a sequence of states  $s_i$ , actions  $a_i$ , and immediate rewards  $r_i$ :  $\tau = (s_0, a_0, r_0, s_1, a_1, r_1, \dots, s_T, a_T, r_T)$ . We denote return-to-go [11]  $R_t$  of trajectory  $\tau$  at the timestep  $t$  as a sum of future rewards from the timestep  $t$  to the end of trajectory:  $R_t = \sum_{t'=t}^T r_{t'}$ . The goal of a reinforcement learning agent is to learn policy  $\pi$  that maximizes the expected return. In online RL, the trajectories used to train an agent are obtained iteratively as the agent interacts with the environment. In offline RL, the agent does not interact with the environment during training. A fixed set of trajectories collected by an arbitrary policy is used for training. Although such a setting is more difficult because it does not allow additional exploration of the environment or generation of new trajectories, it is preferable for tasks where interaction with the environment is costly or risky, such as in robotics.

### 2.2 Partially Observable Markov Decision Process

In the real world, there are frequent situations where the full state of the environment is not available to the agent, so the Markov Property is violated, and the agent is said to receive observations instead of state as input. In this case, observations are no longer sufficient statistics of the past to make a decision in the current step. An example would be a robot navigating an environment based on a camera image or a situation in which a decision must be made based on information from the past that is not available in the current observation. A Partially Observable Markov Decision Process (POMDP) is used in such cases. POMDP is a generalization of the Markov Decision Process (MDP) and is written as  $\langle \mathcal{S}, \mathcal{A}, \mathcal{O}, \mathcal{P}, \mathcal{R}, \mathcal{Z} \rangle$ , where  $o \in \mathcal{O}$  – observations,  $s \in \mathcal{S}$  – states,  $a \in \mathcal{A}$  – actions,  $r = \mathcal{R}(s, a)$  – immediate reward function,  $\mathcal{P}(s'|s, a)$  – state transition function and  $\mathcal{Z}$  is an observation function

$Z_{s',o}^a = P(O = o_{t+1} | S_{t+1} = s', A_t = a)$ . To work successfully in such environments, mechanisms such as memory are needed to allow the use of information from the past. In our work, we propose an approach of adding memory to the agent in the form of memory embeddings and MRV. We consider the formulation of an offline model-free RL, where learning is formulated as a sequence modeling problem [11].

### 3 Recurrent Action Transformer with Memory

In this paper, we introduce a new architecture – **Recurrent Action Transformer with Memory (RATE)** in which we utilized both recurrently trained memory embeddings [8] and the preservation of previous hidden states [16]. A **Memory Retention Valve (MRV)** inside our model allows important information to be carried through sequences many times longer the length of the context. The architecture of RATE is shown in Figure 1.

We used the methodology outlined in the Decision Transformer paper [11] to represent the modeled trajectory. The trajectory is represented as a sequence of triplets  $(R, o, a)$ , where  $R$  denotes the return-to-go,  $o$  represents the observation, and  $a$  signifies the action. The return-to-go  $R_t$  at time step  $t$  corresponds to  $R_t = \sum_{t'=t}^T r_{t'}$ , and the  $R_{t+1}$  at time step  $t + 1$  is obtained from  $R_t$  by subtracting the immediate reward  $r_t$  at time step  $t$ :  $R_{t+1} = \sum_{t'=t+1}^T r_{t'} = R_t - r_t$ . Each component is encoded using the appropriate encoder (Table 6). The memory embeddings, which are model parameters, are inserted at the beginning and end of each segment in the input sequence. This embedded sequence serves as the input for the transformer. The resulting embeddings, obtained in the transformer’s output, correspond to observation vectors that are further employed with linear projection to predict the agent’s action in the respective frame. Memory embedding is a subsequence of  $M$  vectors, where  $M$  is a hyperparameter. These memory embedding subsequences are the same at the beginning and the end of the sequence in the current segment.

During training, we split the trajectories into  $N$  segments of length  $K$ . Thus, instead of the notion of a context  $K$ , we use the notion of an effective context  $K_{eff} = N \times K$  [8], which consists of  $N \times K$  environment steps. We initialize the memory embeddings  $M_0$  with normally distributed random trainable memory vectors. Following a forward pass, we retrieve a new memory embeddings  $\tilde{M}_{n+1}$  from the MRV part of RATE model, which is designed to control the process of forgetting important information. To avoid computational instability, we detach the new memory embeddings. However, the gradient from the next segment can flow to the previous segment through this memory embeddings. We used lower triangular attention masks to attend to tokens within the trajectory sequence. In the case of memory segments, a full attention mask was utilized. Subsequent segments entail updating the memory vectors based on the extracted representations of the suffix memory vectors at the top layer of the transformer. The MRV block also uses a full attention mask when processing memory embeddings.

A sequence of alternately concatenated sequences of memory embeddings  $M_n$ , segment, and memory embeddings  $M_n$  is fed to the RATE input on the segment  $n \in [0, N - 1]$ . As output, we get a sequence of predicted in auto-regressive manner agent’s actions  $\hat{a}_K$  of length  $K$ , used to compute loss, and the updated values of memory embeddings  $\tilde{M}_{n+1}$ , that are input to the RATE input together with the next segment:

$$\hat{a}_K, \tilde{M}_{n+1} = RATE(\text{concat}(M_n, \text{segment}, M_n)) \quad (1)$$

In more detail, the architecture is as follows:

First, we feed a concatenated sequence consisting of memory embeddings and a segment to the input of the Causal Transformer:

$$\hat{a}_K, M_{n+1} = Transformer(\text{concat}(M_n, \text{segment}, M_n)) \quad (2)$$

We obtain the predicted actions  $\hat{a}_K$  used to compute loss, and the updated memory embeddings  $M_{n+1}$ . We then feed these new memory embeddings  $M_{n+1}$  together with those  $M_n$  fed to the Causal Transformer input to the MRV:

$$\tilde{M}_{n+1} = MRV(M_n, M_{n+1}) \quad (3)$$

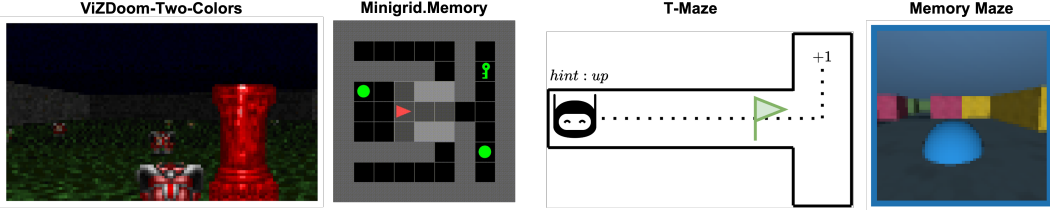


Figure 2: Memory-intensive environments with different observation spaces and reward functions used to test the performance of the memory mechanism in the RATE model.

Thus, we get the final memory embeddings  $\tilde{M}_{n+1}$ , which will be used when processing the next segment. In more detail, inside MRV, we first compute Query, Key and Value matrices using cross-attention:

$$Q_h = M_n W_{q,h}^T, K_h = M_{n+1} W_{k,h}^T, V_h = M_{n+1} W_{v,h}^T \quad (4)$$

Then we use  $\text{Softmax}()$  to process raw attention scores:

$$\tilde{M}_{n+1}^h = \text{Softmax}\left(\frac{Q_h K_h^T}{\sqrt{d_k}}\right) V_h \quad (5)$$

Finally, we combine the matrices obtained for each attention head:

$$\tilde{M}_{n+1} = \text{Linear}(\text{concat}(\tilde{M}_{n+1}^0, \dots, \tilde{M}_{n+1}^h)) \quad (6)$$

Here  $h$  is the head number of the MRV attention heads. In MRV, we use full attention masks.

During inference, actions are predicted in an autoregressive manner:  $t_0 : (R_0, o_0) \rightarrow \text{RATE} \rightarrow a_0$ ;  $t_1 : (R_0, o_0, a_0, R_1, o_1) \rightarrow \text{RATE} \rightarrow a_1 \dots$

## 4 Experimental Evaluation

We designed experiments to accomplish two primary objectives: (a) to demonstrate the success of our RATE model in memory-intensive environments (T-Maze [35], ViZDoom-Two-Colors [46], Memory Maze [38], Minigrid.Memory [12]), and (b) to examine the versatility of the proposed model (Atari games [6] and MuJoCo control tasks [21]). We chose Decision Transformer (DT) [11] as the main baseline for comparison with RATE because it is an offline model that works in the sequence modeling paradigm for RL. It has had many branches [54, 52, 57], can handle both discrete and continuous action spaces, unlike TAP [27], and has no memory mechanism.

### 4.1 Memory-intensive environments

1. **ViZDoom-Two-Colors** [46] – The agent in an acid-filled room observes a quickly disappearing green or red pillar. To stay alive, the agent must recall the pillar’s color and gather items of the same color.
2. **T-Maze** [35] – An agent navigates a T-shaped corridor, receiving a clue at the start about which direction to turn at the end of the corridor. The task tests memory in prolonged environments with sparse rewards, with the agent only receiving a reward at the end.
3. **MemoryMaze** [38] – An agent navigates a maze, seeking objects matching the color of its view frame. The frame color changes after each successful find. The goal is to collect the most matching objects within a time limit.
4. **Minigrid.Memory** [12] – A similar task to T-Maze, but with different observation spaces and reward functions (see Appendix A, Table 4). Another important difference is that the agent appears at a random point at the beginning of the episode, not at the beginning of the corridor. In the case of Minigrid.Memory it is necessary to reach that clue first (in T-Maze it is a memory problem, in Minigrid.Memory it is a memory and credit assignment problem [35]).

For more information about environments, see Appendix A.

In each of the experiments, the RATE configurations were chosen such that the context length  $K$  for the DT was equal to the effective context length  $K_{eff}$  of the RATE. Thus, the actual context length

for RATE was  $N$  times smaller than the DT context length, where  $N$  is the number of segments into which the trajectory is divided. At the same time, RATE and DT process the same trajectory fragments during training. More information about the training procedure for each environment can be found in Appendix C.

In all experiments, we use the same hyperparameters for RATE as for DT for each considered environment to simplify the comparison and listed them in Table 5. Note that the difference between the number of DT and RATE parameters is small:  $\delta p = d\_model \times num\_mem\_tokens \sim 10^3$ .

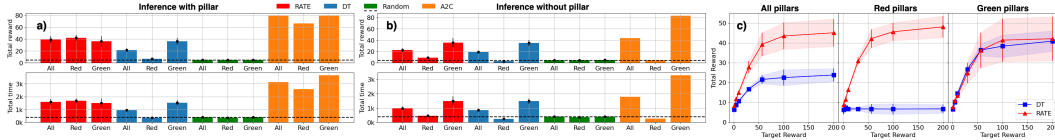


Figure 3: Results for the ViZDoom-Two-Colors with (a) and without (b) pillar in the first 45 steps of the episode. (c) – results of inference as a function of the target return. The training dataset is balanced by the pillar’s color. We demonstrate mean  $\pm$  standard error for 6 runs with 100 seeds.

## 4.2 Experimental Results

**ViZDoom-Two-Colors.** Figure 3 and Figure 4 displays the results for RATE and DT. Results are presented for two configurations of inference: with the pillar visible at the beginning of the episode for the first 45 steps and with the pillar turned off. As can be seen from the left part of the Figure 3, DT is not able to remember the color of the pillar, so the agent has a bias towards green objects (despite the fact that the dataset is balanced). This bias is due to the bias of the original A2C model used to generate the training dataset – A2C model often switches to collecting the green items when red items are to be collected. In turn, RATE successfully remembers the color of the pillar, as reflected in the agent’s ability to collect not only green objects, but also red objects if required.

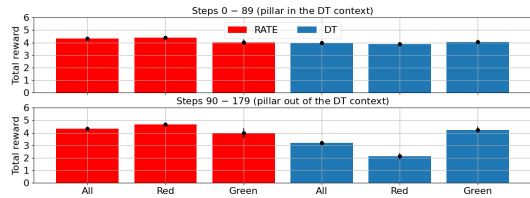


Figure 4: Inference results of RATE and DT at environment steps 0 – 89 (top) and 90 – 179 (bot). dataset – A2C model often switches to collecting the green items when red items are to be collected. At the same time, RATE successfully remembers the color of the pillar, as reflected in the agent’s ability to collect not only green objects, but also red objects if required.

This conclusion of DT’s inability to use information out of context as opposed to RATE is supported by the experimental results presented in Figure 4. The top part of the Figure 4 shows the inference results for the first 90 steps of the environment, when the information about pillar fits completely into the DT context and RATE effective context. In turn, the bottom part shows the inference results for the next 90 environment steps, when the pillar color information starts to disappear from the DT context and RATE effective context (the context window moves as a sliding window). As a result, there is a drop in total reward for red-pillar environments by almost a factor of 2, indicating DT’s inability to memorize information to use it out of context. In turn, for RATE, the values of total reward in the first and second cases are almost unchanged, indicating RATE’s ability to utilize information outside of the current context.

This fact indicates that RATE has indeed remembered the color of the pillar. Furthermore, even in just the first 90 environment steps, divided into  $N = 3$  segments, RATE successfully learns the policy and has an average lifetime of 1700 steps ( $\sim 20$  times more than the number of steps used in training). It is worth noting that it is incorrect to compare RATE and A2C, since RATE is trained offline and A2C is trained online. Figure 3 (c) was constructed to investigate the dependence of model performance on the target reward fed at output. In this paper, we used an empirical estimate of the target reward as the average of the top-10 total rewards in the training dataset.

**T-Maze.** The Figure 5 (a) shows the results of the DT and RATE inference. The inference of these models trained on trajectories of lengths 90 and 150 was conducted on corridor sizes 30 — 900, i.e., much larger than the context length  $K = 30$  of the models. The figure demonstrates that DT’s ability to solve the task is limited by the length of the training data’s context. Specifically, DT-5, trained on trajectories of length  $5 \times 30 = 150$ , exhibits a significant drop in performance (reaching a random turn guessing accuracy of 0.5) when tasked with inference on corridors exceeding 150 in length. This proves that DT-5 struggles to generalize beyond the context it was trained on.

In turn, RATE-3 and RATE-5 (trained on  $3 \times 30 = 90$  and  $5 \times 30 = 150$  steps, respectively) perform significantly better at inference corridor lengths longer than the model saw during training. This confirms the ability of the RATE model to successfully memorize important information and carry it through a long time.

**Minigrid.Memory.** The Figure 5 (d) shows the results of RATE and DT inference in the Minigrid.Memory in mazes of larger size than in the training data, with the context size unchanged. Unlike the previously discussed T-Maze, the credit assignment problem is also solved here, since the agent first has to reach the oracle and find out which object to turn towards in the future. As shown in the Figure 5 (d), RATE significantly outperforms DT for inference at any length.

**Memory Maze.** Despite the lack of policy in the training data, even under the assumption that offline learning does not train the agent to learn exploration, it was possible to obtain better metrics for RATE than for DT. Thus, in terms of mean value  $\pm$  standard error of the mean, the results obtained for 1000 steps of the environment for RATE are  $1.91 \pm 0.10$  and for DT are  $1.45 \pm 0.23$ . Results are shown for 3 model runs at inference at 100 seeds.

The results for Atari and MuJoCo are presented in Table 1 and Table 2. Results for DMamba [36] and MambaDM [9] are from the corresponding papers. A more detailed description of the results obtained can be found in the Appendix C. The authors of MambaDM [9] have not published code at this time, so experiments on memory-intensive environments were not performed.

**Action Associative Retrieval.** As shown above, in experiments with DT in the T-Maze environment, the model has a Success Rate of 50% for inference at corridor lengths longer than the transformer context length. This is due to the fact that even a DT trained on balanced data has a slight bias in the predicted probability towards one of the two required actions, which leads to the fact that when  $t > K$  the agent constantly produces only one target junction action. In turn, the presence of memory in the agent allows us to combat this problem. To test whether an agent has memory in a more explicit way, we design an **Action Associative Retrieval (AAR, Figure 6, Appendix B)** environment.

More formally, we can talk about the presence of memory in an agent when solving AAR (T-Maze-like) tasks under the condition that:

$$\forall t > K : \frac{1}{N_0} \sum_{i=1}^{N_0} p_i(a_t = a^0 | a_0 = a^0) + \frac{1}{N_1} \sum_{i=1}^{N_1} p_i(a_t = a^1 | a_0 = a^1) > 1 \quad (7)$$

Table 1: Raw scores for Atari games for DT and RATE. Results are presented in terms of the mean of 3 runs across 100 seeds  $\pm$  standard deviation. **Green** – top-1 result, **light green** – top-2 result within the standard deviation.

Environment	DT	DMamba	MambaDM	RATE
Breakout	76.9 $\pm$ 27.3	70.6 $\pm$ 9.3	<b>106.9 <math>\pm</math> 5.8</b>	<b>119.8 <math>\pm</math> 15.9</b>
Qbert	2215.8 $\pm$ 1523.7	5786.0 $\pm$ 1295.2	<b>10052.5 <math>\pm</math> 1116.5</b>	<b>12931.4 <math>\pm</math> 820.9</b>
SeaQuest	<b>1129.3 <math>\pm</math> 189.0</b>	<b>992.1 <math>\pm</math> 57.7</b>	<b>1286.0 <math>\pm</math> 42.0</b>	1013.3 $\pm$ 34.6
Pong	<b>17.1 <math>\pm</math> 2.9</b>	1.6 $\pm$ 15.3	<b>18.4 <math>\pm</math> 0.8</b>	<b>18.7 <math>\pm</math> 0.5</b>

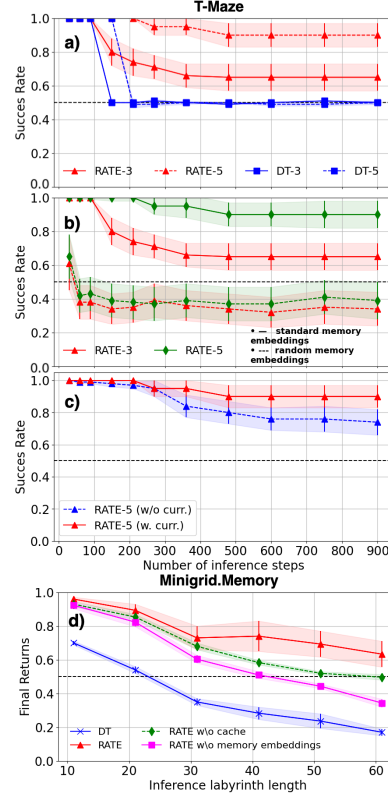


Figure 5: Results for the T-Maze (a, b, c) and Minigrid.Memory (d).

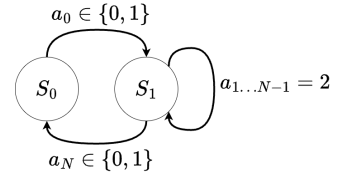


Figure 6: Action Associative Retrieval environment.

Table 2: Scores normalized according to the protocol in [21] for MuJoCo control tasks. ME – Medium-Expert dataset, M – Medium dataset, MR – Medium-Replay dataset. RATE outperforms DT in 9/9 of the cases. **Green** – top-1 result, **light green** – top-2 result within the standard deviation.

Dataset	Environment	CQL	DT	TAP	DMamba	MambaDM	RATE
ME	HalfCheetah	<b>91.6</b>	<b>86.8 ± 1.3</b>	<b>91.8 ± 0.8</b>	<b>91.9 ± 0.6</b>	<b>86.5 ± 1.2</b>	<b>87.4 ± 0.1</b>
ME	Hopper	105.4	107.6 ± 1.8	105.5 ± 1.7	<b>111.1 ± 0.3</b>	<b>110.5 ± 0.3</b>	<b>112.5 ± 0.2</b>
ME	Walker2d	<b>108.8</b>	<b>108.1 ± 0.2</b>	<b>107.4 ± 0.9</b>	<b>108.3 ± 0.5</b>	<b>108.8 ± 0.1</b>	<b>108.7 ± 0.5</b>
M	HalfCheetah	<b>44.4</b>	42.6 ± 0.1	<b>45.0 ± 0.1</b>	42.8 ± 0.1	42.8 ± 0.1	<b>43.5 ± 0.3</b>
M	Hopper	58.0	67.6 ± 1.0	63.4 ± 1.4	<b>83.5 ± 12.5</b>	<b>85.7 ± 7.8</b>	<b>77.4 ± 1.4</b>
M	Walker2d	72.5	74.0 ± 1.4	64.9 ± 2.1	78.2 ± 0.6	78.2 ± 0.6	<b>80.7 ± 0.7</b>
MR	HalfCheetah	<b>45.5</b>	36.6 ± 0.8	<b>40.8 ± 0.6</b>	39.6 ± 0.1	39.1 ± 0.1	39.0 ± 0.6
MR	Hopper	<b>95.0</b>	<b>82.7 ± 7.0</b>	<b>87.3 ± 2.3</b>	<b>82.6 ± 4.6</b>	<b>86.1 ± 2.5</b>	<b>83.7 ± 8.2</b>
MR	Walker2d	<b>77.2</b>	66.6 ± 3.0	66.8 ± 3.1	70.9 ± 4.3	<b>73.4 ± 2.6</b>	<b>73.7 ± 1.4</b>

where  $a^0, a^1 \in \mathcal{A}$  – two mutually exclusive actions leading to a reward;  $t$  is the step at which the final action is required;  $N_0, N_1$  are the number of experiments in environments where target action  $a_t = a^0$  and  $a_t = a^1$ , respectively.

The results of experiments in the AAR environment are presented in Figure 7. The first 1% of training steps was removed because it corresponds to the beginning of the training and is unrepresentative. Blue dots correspond to the beginning of training, red dots to the end of training. As can be seen from Figure 7, during training, the probabilities  $p_i(a_t = a^0 | a_0 = a^0)$  and  $p_i(a_t = a^1 | a_0 = a^1)$  on the training trajectories have a strong positive correlation ( $R_{train}^{DT} = 1.00$  and  $R_{train}^{RATE} = 0.85$ ), where  $R$  – correlation coefficient. This indicates that within-context (effective context) DT and RATE models are able to predict both  $a^0$  and  $a^1$  actions equally well.

At the same time, during validation, for the RATE model this pattern is preserved – the red points corresponding to the probabilities of choosing actions  $a^0$  and  $a^1$  are in the upper right part of the graph, positive correlation persists ( $R_{val}^{RATE} = 0.71$ ). On the other hand, in the DT case, the red cluster of points is shifted towards the probability of choosing action  $a^1$  even when action  $a^0$  is required to be chosen. Thus, in sum, these probabilities are less or equal to 1, as evidenced by a strong negative correlation ( $R_{val}^{DT} = -0.94$ ). The results confirm the inability of DT to generalize on trajectories whose lengths exceed the context length and the ability of RATE to handle such tasks.

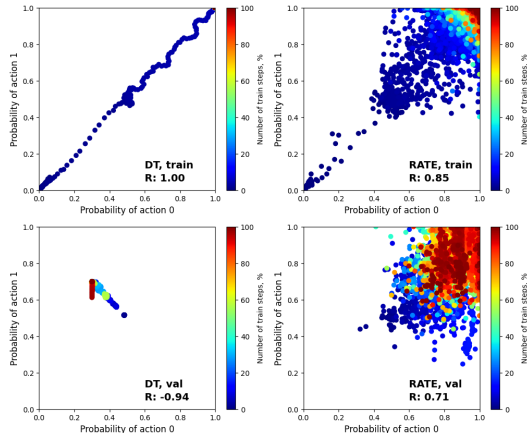


Figure 7: Experimental results with RATE and DT in the AAR environment. The graphs show the 10-runs average results of training on trajectories of length  $T = 90$  and validation on trajectories of length  $T = 180$ , for RATE with  $K_{eff} = 3 \times 30 = 90$  and for DT with  $K = 90$ .

## 5 Ablation Study

In this section, we answer the following questions:

1. "How do the different components of RATE affect model performance in memory-intensive environments?"— Question 1.
2. "What is the benefit of using the curriculum learning? Is its use necessary?"— Question 2.
3. "Why do you need an MRV and what is its best configuration?"— Question 3.

**Question 1. Investigating the impact of RATE components.** To study the influence of memory embeddings on RATE model performance, we conducted the following experiment: for the RATE-3 and RATE-5 models trained for the T-Maze environment (with context  $K = 30$  on  $N = 3$  and  $N = 5$  segments, respectively), we replaced pre-trained memory embeddings with random noise vectors during inference ( Figure 5 (b)). When using random noise instead of memory embeddings, SR = 50%, indicating that the agent successfully reaches the junction, but only takes a turn in one direction regardless of the clue at the beginning of the corridor. Thus, we can conclude that

information about is contained in memory embeddings, while the rest of the actions are shaped by the transformer parameters.

Using the Minigrid.Memory environment, the effect of each of the RATE components on the performance of the model was studied (Figure 5 (d)). So, the inference results shows that the use of memory embeddings and hidden states caching in conjunction with MRV makes the greatest contribution to the performance of the model. Using only cached hidden states or memory embeddings brings a significantly more modest contribution, albeit a positive one.

**Question 2. Curriculum learning.** In the T-Maze environment, the number of actions at the junction relates to the number of actions when moving straight along the corridor as  $\frac{1}{L}$  and tends to 0 as  $L$  increases. In this case, due to the severe imbalance of predicted actions, RATE starts to suffer with predicting rare actions at the junction, but still shows better results compared to DT. This situation can be remedied through curriculum learning. Curriculum learning (CL) is a technique in which a model is trained on examples of increasing difficulty. During the RATE training at T-Maze, it was found that, despite the fact that RATE is able to solve the task with the standard training procedure, using CL allows to get even better results, which is reflected in Figure 5 (c).

**Question 3. Memory Retention Valve architecture ablation.** Without MRV in the T-Maze environment at corridor lengths of  $L \gg K$ , the performance of the RATE model decreased with each segment processed at inference, resulting in  $SR = 50\%$  on long trajectories. For example, in the T-Maze task, the important information to be remembered goes into memory embeddings when processing the first segment of the sequence, and then it must be retrieved when making decisions on the last segment. At the same time, due to the recurrent structure of the architecture, memory embeddings continue to be updated during the processing of intermediate segments when no new information needs to be memorized, causing important information from memory embeddings to leak out. To retain important information in memory embeddings, the Memory Retention Valve (MRV) mechanism was added to the architecture. The 5 different schemes detailed in Appendix E were considered to implement MRV:

1. **MRV-CA-2:** cross-attention-based MRV which uses an attention mechanism to control the updating of memory embeddings and which is used in the work as the main mechanism.
2. **MRV-CA-1:** uses the same mechanism as MRV-CA-2 but the updated memory embeddings  $M_{n+1}$  are fed to Query, and the incoming  $M_n$  are fed to Key and Value.
3. **MRV-G:** gated MRV which uses a gating mechanism similar to the one used in GTrXL [37].
4. **MRV-GRU:** uses a GRU [15] block to process updated  $M_n$  with hidden states.
5. **MRV-LSTM:** uses a LSTM [25] block to process updated  $M_n$  with cached states.

Table 3: Results of ablation study of MRV configuration on T-Maze environment. † – baseline.

Model ( $K_{eff} = 150$ )	Inference corridor length			
	150	360	600	900
RATE w/o MRV†	1.00 ± 0.00	0.66 ± 0.08	0.65 ± 0.07	0.61 ± 0.07
RATE (MRV-CA-2)	1.00 ± 0.00	0.95 ± 0.05	0.90 ± 0.07	0.90 ± 0.07
RATE (MRV-G)	0.86 ± 0.07	0.77 ± 0.08	0.66 ± 0.07	0.65 ± 0.08
RATE (MRV-GRU)	0.99 ± 0.01	0.74 ± 0.07	0.56 ± 0.11	0.55 ± 0.12
RATE (MRV-LSTM)	0.85 ± 0.06	0.64 ± 0.10	0.51 ± 0.11	0.47 ± 0.11
RATE (MRV-CA-1)	0.51 ± 0.01	0.51 ± 0.01	0.49 ± 0.02	0.49 ± 0.01

The best results in their Table 3 are obtained using MRV-CA-2. This configuration is used throughout the work and is denoted simply as MRV.

## 6 Related Work

### 6.1 Transformers for Reinforcement Learning

Transformers have found application in various areas of RL [32, 1]: online RL [37, 29, 20, 58, 33, 48, 40], offline RL [11, 26, 42, 30, 27], and model-based RL model [10, 34, 43]. The use of transformers as a general policy for many environments is also being explored [33, 42, 30]. In our work, we consider the formulation of an offline model-free RL, where learning is formulated as a sequence modeling problem [11]. Prominent representatives of such models are [11, 26, 30,

27], although planning in latent space [27] is considered, which can be seen as modeling of the environment. Moreover, [26, 27] are specialized for control tasks with vector observations and do not generalize to environments with observations in the form of images. Therefore, we consider the Decision Transformer [11], which has no memory mechanism, as the main baseline for comparison.

## 6.2 State Space Models for Reinforcement Learning

Recently, State Space Models (SSMs) [24] have shown significant success in sequence modeling, particularly in offline RL [36, 3, 9, 23]. In Decision S4 (DS4) [3], sequence modeling is executed using S4 layers within the framework of offline RL, whereas Decision Mamba (DMamba) [36] utilizes the most recent Mamba [23] sequence model instead of causal self-attention. Mamba Decision Maker (MambaDM) [9] integrates the unique features of SSMs to effectively combine local and global features with Global-local fusion Mamba (GLOMa) module.

## 6.3 Memory in Transformers

There are many ways to implement the memory mechanism for transformers [16, 41, 18, 51, 31, 53, 8]. In Transformer-XL [16], it is proposed to split a long data sequence into segments and to access past segments at the expense of memory, but to ignore very distant segments. This increases the effective length of the context. The Compressive Transformer [41] uses compressed memory, allowing previous versions of memory to be compressed rather than discarded as in Transformer-XL. ERNIE-Doc [18] suggests using the retrospective feed mechanism and the enhanced recurrence mechanism. Memformer [51] uses external dynamic memory to encode and retrieve past information. MART [31] extends this idea by adding a memory update mechanism similar to a recurrent neural network [25, 13]. The Memorizing Transformer [53] proposes to store the internal representations of past inputs. The Recurrent Memory Transformer [8] includes additional read and write memory tokens at each segment’s beginning and end. This method allows the effective context to be expanded to over 1 million tokens [59]. Our work is the first attempt to adapt transform models with memory to generate agent actions in various reinforcement learning tasks in the Offline-RL setting. An Adaptive Agent (AdA) [4] uses memory architectures to store and employ information previously acquired by the agent. The default memory architecture is Transformer-XL [16] with normalization before each layer [37], and the use of gating on the feedforward layers [45] to stabilize training. We also use Transformer-XL in our work but refrain from using additional modifications to stabilize training. Another distinctive feature of using a transformer in AdA, as opposed to DT, is that pixel observations, past actions, past rewards, and additional information are not tokenized separately but are combined into a single vector that feeds the transformer. The transformer itself predicts not only actions but also value function values.

## 7 Conclusion

In this paper, we propose the **Recurrent Action Transformer with Memory (RATE)**, an autoregressive transformer model for offline reinforcement learning problems that exploits the mechanisms of recurrent memory and **Memory Retention Valve (MRV)** that control memory updating. In extensive experiments on environments such as ViZDoom-Two-Colors, Memory Maze, Minigrid.Memory and T-Maze, we have shown that RATE outperforms models without recurrent memory. We also show that the proposed model achieves better or comparable results against SOTA Mamba-based models in Atari and MuJoCo environments, confirming its versatility. We thoroughly investigated the influence of memory mechanisms on the model’s performance and showed that the model does indeed use them when making a decision. This method shows great potential for tackling complex tasks involving long sequences, particularly in robotics where training agents on pre-collected datasets is highly beneficial.

**Limitations.** When it comes to modeling short sequences where all the data fits into the context of a transformer, the RATE model is of limited use. In these cases, the effectiveness of the memory mechanisms is limited because there is no need for processing long dependencies, which allows the use of a common transformer.

**Impact Statements.** In this paper, we present research intended to further the development of machine learning. There are many potential societal effects of our work, but we believe that none need special emphasis in this discussion.

## References

- [1] Pranav Agarwal et al. “Transformers in reinforcement learning: a survey”. In: *arXiv preprint arXiv:2307.05979* (2023).
- [2] Rishabh Agarwal, Dale Schuurmans, and Mohammad Norouzi. “An optimistic perspective on offline reinforcement learning”. In: *International Conference on Machine Learning*. PMLR, 2020, pp. 104–114.
- [3] Shmuel Bar-David et al. “Decision s4: Efficient sequence-based rl via state spaces layers”. In: *arXiv preprint arXiv:2306.05167* (2023).
- [4] Jakob Bauer et al. “Human-Timescale Adaptation in an Open-Ended Task Space”. In: *Proceedings of the 40th International Conference on Machine Learning*. Ed. by Andreas Krause et al. Vol. 202. Proceedings of Machine Learning Research. PMLR, 23–29 Jul 2023, pp. 1887–1935. URL: <https://proceedings.mlr.press/v202/bauer23a.html>.
- [5] Edward Beeching et al. “Deep Reinforcement Learning on a Budget: 3D Control and Reasoning Without a Supercomputer”. In: *CoRR abs/1904.01806* (2019). arXiv: 1904.01806. URL: <http://arxiv.org/abs/1904.01806>.
- [6] Marc G Bellemare et al. “The arcade learning environment: An evaluation platform for general agents”. In: *Journal of Artificial Intelligence Research* 47 (2013), pp. 253–279.
- [7] Iz Beltagy, Matthew E Peters, and Arman Cohan. “Longformer: The long-document transformer”. In: *arXiv preprint arXiv:2004.05150* (2020).
- [8] Aydar Bulatov, Yury Kuratov, and Mikhail Burtsev. “Recurrent memory transformer”. In: *Advances in Neural Information Processing Systems* 35 (2022), pp. 11079–11091.
- [9] Jiahang Cao et al. “Mamba as Decision Maker: Exploring Multi-scale Sequence Modeling in Offline Reinforcement Learning”. In: *arXiv preprint arXiv:2406.02013* (2024).
- [10] Chang Chen et al. “Transdreamer: Reinforcement learning with transformer world models”. In: *arXiv preprint arXiv:2202.09481* (2022).
- [11] Lili Chen et al. “Decision transformer: Reinforcement learning via sequence modeling”. In: *Advances in neural information processing systems* 34 (2021), pp. 15084–15097.
- [12] Maxime Chevalier-Boisvert et al. “Minigrid & Miniworld: Modular & Customizable Reinforcement Learning Environments for Goal-Oriented Tasks”. In: *CoRR abs/2306.13831* (2023).
- [13] Kyunghyun Cho et al. “On the properties of neural machine translation: Encoder-decoder approaches”. In: *arXiv preprint arXiv:1409.1259* (2014).
- [14] Krzysztof Choromanski et al. “Rethinking attention with performers”. In: *arXiv preprint arXiv:2009.14794* (2020).
- [15] Junyoung Chung et al. “Empirical evaluation of gated recurrent neural networks on sequence modeling”. In: *arXiv preprint arXiv:1412.3555* (2014).
- [16] Zihang Dai et al. “Transformer-xl: Attentive language models beyond a fixed-length context”. In: *arXiv preprint arXiv:1901.02860* (2019).
- [17] Jiayu Ding et al. “Longnet: Scaling transformers to 1,000,000,000 tokens”. In: *arXiv preprint arXiv:2307.02486* (2023).
- [18] Siyu Ding et al. “ERNIE-Doc: A retrospective long-document modeling transformer”. In: *arXiv preprint arXiv:2012.15688* (2020).
- [19] Yan Duan et al. “RL2: Fast reinforcement learning via slow reinforcement learning”. In: *arXiv preprint arXiv:1611.02779* (2016).
- [20] Kevin Esslinger, Robert Platt, and Christopher Amato. “Deep Transformer Q-Networks for Partially Observable Reinforcement Learning”. In: *arXiv preprint arXiv:2206.01078* (2022).
- [21] Justin Fu et al. *D4RL: Datasets for Deep Data-Driven Reinforcement Learning*. 2021. arXiv: 2004.07219 [cs.LG].
- [22] Jake Grigsby, Linxi Fan, and Yuke Zhu. “AMAGO: Scalable In-Context Reinforcement Learning for Adaptive Agents”. In: *The Twelfth International Conference on Learning Representations*. 2024. URL: <https://openreview.net/forum?id=M6XWoEdmwf>.
- [23] Albert Gu and Tri Dao. “Mamba: Linear-time sequence modeling with selective state spaces”. In: *arXiv preprint arXiv:2312.00752* (2023).
- [24] Albert Gu, Karan Goel, and Christopher Ré. “Efficiently modeling long sequences with structured state spaces”. In: *arXiv preprint arXiv:2111.00396* (2021).

- [25] Sepp Hochreiter and Jürgen Schmidhuber. “Long short-term memory”. In: *Neural computation* 9.8 (1997), pp. 1735–1780.
- [26] Michael Janner, Qiyang Li, and Sergey Levine. “Offline reinforcement learning as one big sequence modeling problem”. In: *Advances in neural information processing systems* 34 (2021), pp. 1273–1286.
- [27] Zhengyao Jiang et al. “Efficient Planning in a Compact Latent Action Space”. In: *The Eleventh International Conference on Learning Representations*. 2023. URL: <https://openreview.net/forum?id=cA77NrVEuqn>.
- [28] Jikun Kang et al. “Think before you act: Decision transformers with internal working memory”. In: *arXiv preprint arXiv:2305.16338* (2023).
- [29] Andrew Lampinen et al. “Towards mental time travel: a hierarchical memory for reinforcement learning agents”. In: *Advances in Neural Information Processing Systems* 34 (2021), pp. 28182–28195.
- [30] Kuang-Huei Lee et al. “Multi-game decision transformers”. In: *Advances in Neural Information Processing Systems* 35 (2022), pp. 27921–27936.
- [31] Jie Lei et al. “Mart: Memory-augmented recurrent transformer for coherent video paragraph captioning”. In: *arXiv preprint arXiv:2005.05402* (2020).
- [32] Wenzhe Li et al. “A Survey on Transformers in Reinforcement Learning”. In: *Transactions on Machine Learning Research* (2023). Survey Certification. ISSN: 2835-8856. URL: <https://openreview.net/forum?id=r30yuDPvf2>.
- [33] Luckeciano C Melo. “Transformers are meta-reinforcement learners”. In: *International Conference on Machine Learning*. PMLR. 2022, pp. 15340–15359.
- [34] Vincent Micheli, Eloi Alonso, and François Fleuret. “Transformers are Sample-Efficient World Models”. In: *The Eleventh International Conference on Learning Representations*. 2023. URL: <https://openreview.net/forum?id=vhFu1Acb0xb>.
- [35] Tianwei Ni et al. “When Do Transformers Shine in RL? Decoupling Memory from Credit Assignment”. In: *Thirty-seventh Conference on Neural Information Processing Systems*. 2023. URL: <https://openreview.net/forum?id=APGXBNkt6h>.
- [36] Toshihiro Ota. “Decision mamba: Reinforcement learning via sequence modeling with selective state spaces”. In: *arXiv preprint arXiv:2403.19925* (2024).
- [37] Emilio Parisotto et al. “Stabilizing transformers for reinforcement learning”. In: *International conference on machine learning*. PMLR. 2020, pp. 7487–7498.
- [38] Jurgis Pasukonis, Timothy Lillicrap, and Danijar Hafner. “Evaluating Long-Term Memory in 3D Mazes”. In: *arXiv preprint arXiv:2210.13383* (2022).
- [39] Marco Pleines et al. “TransformerXL as Episodic Memory in Proximal Policy Optimization”. In: *Github Repository* (2023). URL: <https://github.com/MarcoMeter/episodic-transformer-memory-ppo>.
- [40] Subhojeet Pramanik et al. “Recurrent Linear Transformers”. In: *arXiv preprint arXiv:2310.15719* (2023).
- [41] Jack W Rae et al. “Compressive transformers for long-range sequence modelling”. In: *arXiv preprint arXiv:1911.05507* (2019).
- [42] Scott Reed et al. “A generalist agent”. In: *arXiv preprint arXiv:2205.06175* (2022).
- [43] Jan Robine et al. “Transformer-based World Models Are Happy With 100k Interactions”. In: *The Eleventh International Conference on Learning Representations*. 2023. URL: <https://openreview.net/forum?id=TdBaDGCpjly>.
- [44] John Schulman et al. “Proximal policy optimization algorithms”. In: *arXiv preprint arXiv:1707.06347* (2017).
- [45] Noam Shazeer. “Glu variants improve transformer”. In: *arXiv preprint arXiv:2002.05202* (2020).
- [46] Artyom Sorokin et al. “Explain My Surprise: Learning Efficient Long-Term Memory by Predicting Uncertain Outcomes”. In: (July 2022). DOI: 10.48550/arXiv.2207.13649.
- [47] R.S. Sutton and A.G. Barto. *Reinforcement Learning, second edition: An Introduction*. Adaptive Computation and Machine Learning series. MIT Press, 2018. ISBN: 9780262039246. URL: <https://books.google.ru/books?id=sWVODwAAQBAJ>.
- [48] Adaptive Agent Team et al. “Human-timescale adaptation in an open-ended task space”. In: *arXiv preprint arXiv:2301.07608* (2023).

- [49] Ashish Vaswani et al. “Attention is all you need”. In: *Advances in neural information processing systems* 30 (2017).
- [50] Jane X Wang et al. “Learning to reinforcement learn”. In: *arXiv preprint arXiv:1611.05763* (2016).
- [51] Qingyang Wu et al. “Memformer: The memory-augmented transformer”. In: *arXiv preprint arXiv:2010.06891* (2020).
- [52] Yueh-Hua Wu, Xiaolong Wang, and Masashi Hamaya. “Elastic decision transformer”. In: *Advances in Neural Information Processing Systems* 36 (2024).
- [53] Yuhuai Wu et al. “Memorizing transformers”. In: *arXiv preprint arXiv:2203.08913* (2022).
- [54] Taku Yamagata, Ahmed Khalil, and Raul Santos-Rodriguez. “Q-learning Decision Transformer: Leveraging Dynamic Programming for Conditional Sequence Modelling in Offline RL”. In: *Proceedings of Machine Learning Research* 202 (23–29 Jul 2023). Ed. by Andreas Krause et al., pp. 38989–39007. URL: <https://proceedings.mlr.press/v202/yamagata23a.html>.
- [55] Manzil Zaheer et al. “Big bird: Transformers for longer sequences”. In: *Advances in neural information processing systems* 33 (2020), pp. 17283–17297.
- [56] Susan Zhang et al. “Opt: Open pre-trained transformer language models”. In: *arXiv preprint arXiv:2205.01068* (2022).
- [57] Qinqing Zheng, Amy Zhang, and Aditya Grover. “Online Decision Transformer”. In: *Proceedings of Machine Learning Research* 162 (17–23 Jul 2022). Ed. by Kamalika Chaudhuri et al., pp. 27042–27059. URL: <https://proceedings.mlr.press/v162/zheng22c.html>.
- [58] Qinqing Zheng, Amy Zhang, and Aditya Grover. “Online decision transformer”. In: *international conference on machine learning*. PMLR, 2022, pp. 27042–27059.
- [59] Xizhou Zhu et al. “Deformable detr: Deformable transformers for end-to-end object detection”. In: *arXiv preprint arXiv:2010.04159* (2020).

## A Environments

### A.1 Memory-intensive environments

**ViZDoom-Two-Colors.** We used a modified ViZDoom-Two-Colors environment from [46] to assess the model’s memory abilities. The agent initially having 100 hit points (HP) is placed in a room without inner walls filled with acid. At each step in the environment, the agent loses a fixed amount of health (5/32 HP per step). In the center of the environment, there is a pillar of either green or red color, which disappears after 45 environment steps. Throughout the environment, objects of two colors (green and red) are generated. When the agent interacts with an object of the same color as the pillar, it gains an increase in health of +25 and a reward of +1. When the agent interacts with an object of the opposite color, it loses a similar amount of health. The agent receives an additional reward of +0.01 for each step it survives. The episode ends when the agent has zero health. Thus, the agent needs to remember the color of the pillar to select items of the correct color, even if the pillar is out of sight or has disappeared. The agent does not receive information about its current health or rewards, as these observations essentially convey the same information as the color of the pillar but persist beyond step 45. We collected a dataset of 5000 trajectories of 90 steps in length using a trained A2C agent [5] (an agent trained with a non-disappearing pillar). When collecting trajectories, to ensure that the agent saw the pillar before it disappeared, the agent always appeared facing the pillar in the same place – midway between the pillar and the nearest wall. In order to successfully complete this task, the agent needs to remember the color of the pillar. This environment tests the long-term memory mechanism, since the agent needs to retain information about the pillar for a time much longer than the pillar has been in the environment. Using only short-term memory and, for example, collecting the next item of the same color as the previous collected item, it will not be possible for the agent to survive for a long time, as this policy is extremely unstable. This is due to the fact that in the training dataset the agent occasionally makes a mistake and picks up an object of the opposite color. Thus, irrelevant information about the desired color may enter the transformer context and the agent will start collecting items of an opposite color, which will quickly lead to a failure.

**T-Maze.** To investigate agent’s long-term memory on very long environments (the inference trajectory length is much longer than the context length  $K$ ) we used a modified version of the T-Maze environment [35]. The agent’s objective in this environment is to navigate from the beginning of the T-shaped maze to the junction and choose the correct direction, based on a signal given at the beginning of the trajectory using four possible actions  $a \in \{left, up, right, down\}$ . This signal, represented as the *clue* variable and equals to zero everywhere except the first observation, dictates whether the agent should turn up ( $clue = 1$ ) or down ( $clue = -1$ ). Additionally, a constraint on the episode duration  $T = L + 2$ , where the maximum duration is determined by the length of the corridor  $L$  to the junction, adds complexity to the problem. To address this, a binary flag, represented as the *flag* variable, which is equal to 1 one step before the junction and 0 otherwise, indicating the arrival of the agent at the junction, is included in the observation vector. Additionally, a noise channel is added to the observation vector, with random integer values from the set  $\{-1, 0, +1\}$ . The observation vector is thus defined as  $o = [y, clue, flag, noise]$ , where  $y$  represents the vertical coordinate. The reward  $r$  is given only at the end of the episode and depends on the correctness of the agent’s turn at the junction, being 1 for a correct turn and 0 otherwise. This formulation deviates from the traditional Passive T-Maze environment [35] (different observations and reward functions) and presents a more intricate set of conditions for the agent to navigate and learn within the given time constraint.

**Memory Maze.** In this first-person view 3D environment [38], the agent appears in a randomly generated maze containing several objects of different colors at random locations. The agent’s task is to find an object of the same color in the maze as the outline around its observation image. After the agent finds an object of the desired color and steps on it, the color of the outline changes and the agent must find another object. The agent receives a +1 reward for stepping on the correct object. Otherwise, he receives no reward. The duration of an episode is a fixed number and is equal to 1000. Thus, the agent’s task is to find as many objects of the desired color as possible in a limited time. The agent’s effectiveness in this environment depends on its ability to memorize the structure of the maze and the location of objects in it in order to find the desired objects faster.

**Minigrid.Memory.** Minigrid.Memory [12] is a 2D grid environment designed to test an agent’s long-term memory and credit-assignment [35]. The environment map is a T-shaped maze with a small room with an object inside it at the beginning. The agent appears at a random coordinate in the maze. The agent’s task is to reach the room with the object and memorize it, then reach the junction at the end of the maze and make a turn in the direction where the same object is located as in the room at the beginning of the maze. A reward  $r_t = 1 - 0.9 \times \frac{t}{T}$  is given for success, and 0 for failure. The episode ends after any agent turns at a junction or after a limited amount of time (95 steps) has elapsed. The agent’s observations are limited to a  $3 \times 3$  size frame.

## A.2 Standard benchmarks

**Atari games.** For the Atari game environments [6], we used the same dataset as in DT, namely the DQN replay dataset with grayscale state images [2]. This dataset contains 500 thousand of the 50 million steps of an online DQN agent for each game. We use the following set of games: SeaQuest, Breakout, Pong and Qbert.

**MuJoCo.** Despite the fact that memory is not explicitly used in decision making in control environments like MuJoCo [21], we conducted additional experiments in this environment to compare with DT. For the continuous control tasks, we selected a standard MuJoCo locomotion environment and a set of trajectories from the D4RL benchmark [21]. Since we chose DT and TAP as the main models for comparison on this data, we focused on the environments used in both works (HalfCheetah, Hopper, and Walker). We used three different dataset settings: 1) **Medium** – 1 million timesteps generated by a “medium” policy that achieves about a third of the score of an expert policy; 2) **Medium-Replay** – the replay buffer of an agent trained with the performance of a medium policy (about 200k–400k timesteps in our environments); 3) **Medium-Expert** – 1 million timesteps generated by the medium policy concatenated with 1 million timesteps generated by an expert policy. The scores for the MuJoCo experiments are normalized such that 100 represents an expert policy, following the benchmark protocol outlined in [21]. The performance metrics for CQL and TAP are reported from the TAP paper [27], and for DT from the DT paper [11], as they use the same dataset and evaluation protocol.

Table 4: Description of observations and reward functions for the considered environments.  
\* – discrete for the Atari.Pong.

Environment	Obs. type	Rewards	Actions	Obs. info
ViZDoom-Two-Colors	Image	Continuous	Discrete	First-person view
T-Maze	Vector	Sparse & Discrete	Discrete	Vector
Memory Maze	Image	Sparse & Discrete	Discrete	First-person view
Minigrid.Memory	Image	Continuous	Discrete	Observes the $3 \times 3$ part of the grid
Atari	Image	Continuous*	Discrete	Observes the full game screen
MuJoCo	Vector	Continuous	Continuous	Vector

## B Action Associative Retrieval

There are two states in this environment:  $S_0$  and  $S_1$ . The agent appears in state  $S_0$  and by performing the action  $a_0 \in \{0, 1\}$  moves to state  $S_1$ . Next, the agent must take  $N - 2$  steps to move from state  $S_1$  to state  $S_1$  by performing action  $a = 2$  (no op.). At the end of the episode, the agent must perform the same action that moved it from state  $S_0$  to state  $S_1$  in order to move from state  $S_1$  to state  $S_0$ . Thus, the action  $a \in \{0, 1, 2\}$ . Agent observations  $o = [state, flag, noise]$ , where  $state \in \{0, 1\}$  is the index of the current state,  $flag \in \{0, 1\}$  is a flag equal to 1 in case the next step requires returning to the initial state and equal to 0 otherwise,  $noise \in \{-1, 0, +1\}$  is the noise channel. The agent receives a +1 reward if it returns to the initial state  $S_0$  by performing the action that took it out from the  $S_0$  to the  $S_1$ , and  $-1$  in other cases.

## C Training

**ViZDoom-Two-Colors.** To train RATE on this environment, we collected dataset of 5000 trajectories of length 90 environment steps using a pre-trained A2C agent (trained without disappearing oh the pillar) [5]. Since the pillar disappears at time  $t = 45$ , all trajectories start at time  $t = 0$  and end at time  $t = 90$  so that the information about the color of the pillar is guaranteed to be used in training. In this experiment, we compared DT with context length  $K = 90$  to our RATE model with context length  $K = 30$  and partitioning the trajectory into  $N = 3$  segments. Thus, when trained, RATE also handles sequences of length 90, since its effective context is  $K_{eff} = N \times K = 90$ , but only processed subsequences of length  $K = 30$ .

**T-Maze.** The model names are written in the format MODEL-N, where  $N$  is the number of segments of length  $K = 30$  into which the training trajectories can be partitioned. Thus, DT-3 was trained on trajectories of length  $T \leq 3 \times 30 = 90$ , and DT-5 was trained on trajectories of length  $T \leq 5 \times 30 = 150$  with context lengths  $K = 90$  and  $K = 150$ , respectively. RATE-3 and RATE-5 were trained on similar trajectories as DT-3 and DT-5, but with each trajectory divided into 3 and 5 segments, respectively, during training, enabling the training of a model with a context length of  $K = 30$  on trajectories of length  $T = 90$  and  $T = 150$ . On this environment, RATE was trained using curriculum learning because this approach produces better results. However, it is important to note that the T-Maze task is successfully solved by the RATE model without using curriculum learning (see section 5 for details). All the trajectories used in training start from  $t = 0$ , i.e., from the moment of receiving a clue. The work showed that the use of Curriculum Learning (CL) allows one to achieve significantly better results when solving the T-Maze environment. In this approach, the model is first trained on the set of trajectories  $Q_1 = q_1$  of length  $K \times 1$ , then the trained model is re-trained on the set of trajectories  $Q_2 = q_1 \cup q_2$ , where the set  $q_2$  is formed by trajectories of length  $K \times 2$ , and so on (in order of increasing complexity of the trajectories). Thus, for the  $N$  segments considered during training, the set  $Q_N = \bigcup_{i=1}^N q_i$  is used.

**Memory Maze.** To train DT and RATE on Memory Maze, the same approach was used as for ViZDoom-Two-Colors environment, except that trajectories were sampled not from  $t = 0$  but from  $t : \sum_{t'=t}^{t+90} r_{t'} \geq 2$ . This is because in the [38] offline training data posted by the authors, the average value of the total reward over all trajectories where the total reward is  $> 0$  is 1.06. Furthermore, the trajectories themselves are not collected by an agent with an optimal or suboptimal policy, but by an agent navigating to a random object in the maze. As in the ViZDoom-Two-Colors case, training for DT was performed with a context length of  $K = 90$  and for RATE with a context length of  $K = 30$  and number of segments  $N = 3$ , i.e., effective context length  $K_{eff} = N \times K = 3 \times 30 = 90$ .

**Minigrid.Memory.** To train RATE and DT on this environment, trajectories were sampled in the same manner as for T-Maze. An environment configuration with a maze of size  $13 \times 13$  was used as a basis, and trajectories were collected using PPO [44] with TransformerXL [39] with a context length equal to the maximum episode duration. Since the maximum episode duration is 95, training proceeded in the following setting: for DT the context length  $K = 30$ , for RATE the context length  $K = 10$  and the number of segments  $N = 3$ . All trajectories, as in T-Maze, are sampled from time  $t = 0$ .

**Atari and MuJoCo.** When training RATE on Atari games and MuJoCo control tasks, sequences of length  $T = 90$  (Atari) and  $T = 60$  (MuJoCo) were sampled randomly from the original trajectories in the dataset. These trajectories were then divided into  $N = 3$  segments of length  $K = 30$  (Atari) and  $K = 20$  (MuJoCo), forming an effective context of length  $K_{eff} = N \times K = 90$  (60 for the MuJoCo).

For the Atari, we used the identical experimental design described in the DT paper [11]. It is worth noting that we presented raw scores for Atari, rather than gamer-normalized scores as described in the DT paper. Table 1 shows the results for Atari environments. RATE outperforms DT significantly in environments like Breakout and Qbert. We attribute this to the observation that, although these environments do not explicitly demand memory, intricate dynamics from the past exert a greater influence on agent behavior than in environments such as SeaQuest. Actions executed in the past notably alter the present state of the environment in Breakout and Qbert, whereas in SeaQuest, such

actions hold little significance. For instance, the emergence of enemies and divers in SeaQuest is entirely independent of the agent’s prior actions.

For the MuJoCo, our findings suggest that the conventional strategy of utilizing return is not suitable for our segment-based scheme. The issue arises during the trajectory, where the agent’s return persistently diminishes. However, the true value of the agent’s state at the onset and conclusion of the episode could remain unchanged, provided the agent’s policy performs consistently well. To rectify this discrepancy, we propose a novel evaluation strategy for MuJoCo tasks. In this approach, each segment commences with the maximum return, simulating the scenario where the agent initiates the trajectory anew. This method effectively mitigates the aforementioned issue, enhancing the accuracy of our evaluation process. Our MuJoCo experiments in Table 2 show that this benefits performance significantly for some environments. Thus, using RATE allowed us to obtain the best metrics for MuJoCo in 5/9 cases compared to the other baselines. RATE also outperforms DT in 9/9 tasks.

## D Hyperparameters

In this section, Table 5 lists the hyperparameters used to train the RATE model. Inside the Memory Retention Valve, the number of attention heads = 2 was used for all environments (with the exception of Memory Maze, for which this parameter is set to 4).

Table 5: RATE hyperparameters for different experiments. ‡ – Leaky ReLU in the Atari.Pong case.

Hyperparameter	ViZDoom2C / Memory Maze	T-Maze / Minigrid.Memory	Atari	MuJoCo
Number of layers	6	8	6	3
Number of attention heads	8	10	8	1
Embedding dimension	128	64	128	128
Context length K	30	30 / 10	30	20
Number of segments	3	3	3	3
Hidden dropout	0.2	0.05 / 0.2	0.2	0.2
Attention dropout	0.05	0 / 0.05	0.05	0.05
Number of memory tokens	15	5	15	15
Max epochs	1000	250	10	10
Batch size	128	64	128	4096
Weight decay	0.1	1e-4	0.1	0.1
Loss function	CE	CE	CE	MSE
Optimizer	AdamW	AdamW	AdamW	AdamW
MRV activation	ReLU	ReLU	ReLU‡	ReLU
MRV number of attention heads	2 / 4	2	2	2

Table 6: RATE encoders for each part of  $(R, o, a)$  triplets. We use Embedding layer for encoding discrete actions and Linear for continuous ones. ‡ – channels / kernel sizes / padding.

Env.	R	O	Conv. configuration‡	A
ViZDoom-Two-Colors	Linear	Conv2D $\times$ 3	(32, 64, 64) / (8, 4, 3) / 0	Embedding
T-Maze	Linear	Linear	–	Embedding
Memory Maze	Linear	Conv2D $\times$ 3	(32, 64, 64) / (8, 4, 3) / 2	Embedding
Minigrid.Memory	Linear	Conv2D $\times$ 3	(32, 64, 64) / (8, 4, 3) / 0	Embedding
Atari	Linear	Conv2D $\times$ 3	(32, 64, 64) / (8, 4, 3) / 0	Embedding
MuJoCo	Linear	Linear	–	Linear

## E Memory Retention Valve

The MRV-G scheme was inspired by the gating mechanism from GTrXL [37] and implemented as follows:

$$r = \sigma(M_n W_r + M_{n+1} U_r) \tag{8}$$

$$z = \sigma(M_n W_z + M_{n+1} U_z - bias) \tag{9}$$

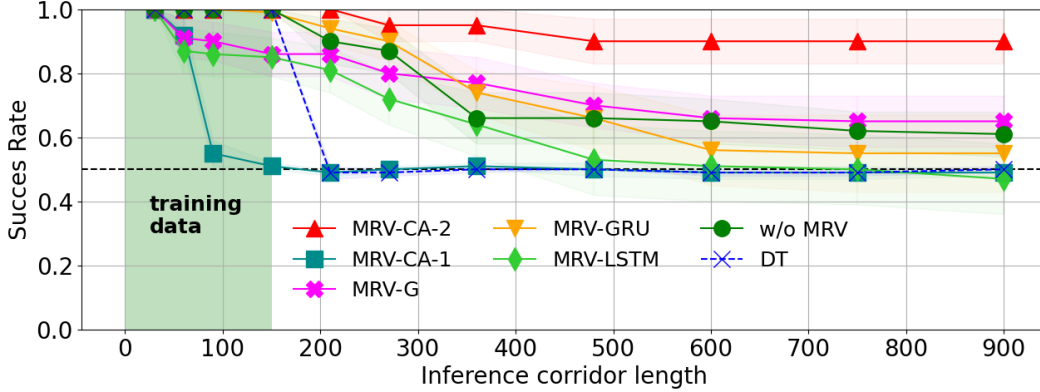


Figure 8: Results of RATE inference with different MRV configurations on the T-Maze environment. Training was performed with the number of segments  $N = 5$  and context length  $K = 30$ , i.e. on trajectories of length  $\leq 150$ . MRV-CA-2 is the final MRV configuration that is used throughout the work and is designated as MRV.

$$h = \tanh(M_n W_g + (M_{n+1} \times r) U_r) \quad (10)$$

$$\tilde{M}_{n+1} = \sigma(M_n(1 - z) + z \times h) \quad (11)$$

The results of the RATE (trained on corridor lengths of  $\leq 150$ ) inference on the T-Maze environment with these MRV configurations are shown in Figure 8 and in Table 3.

## F Technical details

The Table 7 shows the technical parameters of the training models. Note that the difference between the number of DT and RATE parameters is small and equal to  $\delta p = d_{\text{model}} \times \text{num\_mem\_tokens} \sim 10^3$ . Training RATE with trajectory splitting into  $N$  segments allows  $\sim N$  smaller GPU memory size usage than for DT. The training was conducted using a single NVIDIA Tesla A100 80 Gb graphics card.

The code is available at <https://github.com/AIRI-Institute/RATE>.

Table 7: Technical configurations of model training. The values in the table are for single run. The training was conducted on a single Nvidia A100 GPU.

Env.	Model	GPU mem.	Train time	# params.
ViZDoom-Two-Colors	RATE	10Gb	4h	6.0M
	DT	30Gb		
T-Maze	RATE	10Gb	2h	2.4M
	DT	15Gb		
Memory Maze	RATE	10Gb	12h	6.0M
	DT	30Gb		
Minigrid.Memory	RATE	6Gb	10h	6.0M
	DT	15Gb		
Atari	RATE	11.5Gb	9h	4.7M
	DT	32Gb		
MuJoCo	RATE	15Gb	10h	0.6M
	DT	45Gb		

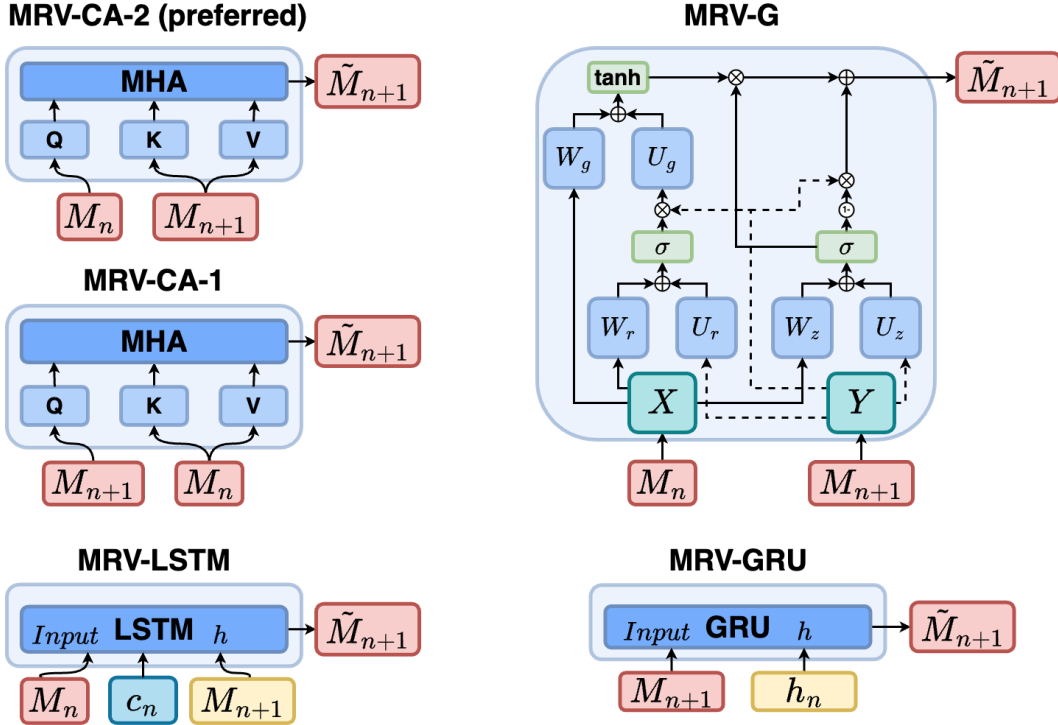


Figure 9: Memory Retention Valve configurations used in the ablation study. **MRV-CA-2**: cross-attention-based MRV which uses an attention mechanism to control the updating of memory embeddings and which is used in the work as the main mechanism. **MRV-CA-1**: uses the same mechanism as MRV-CA-2 but the updated memory embeddings  $M_{n+1}$  are fed to Query, and the incoming memory embeddings  $M_n$  are fed to Key and Value. **MRV-G**: gated MRV which uses a gating mechanism similar to the one used in Gated Transformer-XL [37]. **MRV-GRU**: uses a GRU [15] block to process updated memory embeddings with hidden states. **MRV-LSTM**: uses a LSTM [25] block to process updated memory embeddings with cached states.